

# Microstructural Evolution and Growth of Crystallite Size of Mullite During Thermal Transformation of Kyanite

M. A. Sainz,<sup>a</sup> F. J. Serrano,<sup>b</sup> J. Bastida<sup>b</sup> and A. Caballero<sup>a</sup>

<sup>a</sup>Instituto de Cerámica y Vidrio, C.S.I.C., 28500 Arganda del Rey, Madrid, Spain

<sup>b</sup>Departamento de Geología, Universidad de Valencia (E.G.), 46100 Burjassot, Valencia, Spain

(Received 26 March 1996; revised version received 10 November 1996; accepted 11 November 1996)

## Abstract

*The microstructural evolution of mullite during the thermal transformation of kyanite has been studied in the temperature range 1200–1600°C. The shape and size of the grains were analysed by means of SEM-EDS while crystallite size evolution was studied by X-ray line profile analyses.*

*The results obtained showed that total transformation of kyanite to mullite takes place between 1350 and 1400°C. At temperatures below 1350°C needle-like mullite grains are always produced. At higher temperatures the mullite grains reveal rounded end platelet morphology. Evolution from needle-like to platelet shape was correlated with the X-ray data.*

© 1997 Elsevier Science Limited.

## 1 Introduction

In the last decade, the need to produce high-quality mullite for optical, dielectric and structural applications, has led to numerous studies on the synthesis and processing of mullite.<sup>1</sup> There are several manufacturing methods:<sup>2</sup> sol-gel, coprecipitation, alkoxide, spray pyrolysis, hydrothermal synthesis, etc. On the other hand, starting with cheap raw materials (kaolin, kaolin plus alumina, sillimanite minerals, etc.) it is also possible to produce high-purity mullite, and properties obtainable through conventional ceramic processing and firing are outstanding.

The purpose of the present work was to study the microstructural evolution of mullite during thermal transformation of kyanite. The results obtained showed that acicular or rounded end platelet mullite grains of controlled size, with composition close to theoretical mullite, could be obtained.

X-Ray diffraction (XRD) line broadening is caused by specimen and experimental factors. Within the former, the small size of crystal domains (crystallites) and the lattice strains of the specimen are the two main causes for line broadening, whereas wavelength distribution and geometric instrumental aberrations are the other factors that contribute to line broadening. Size and strain parameters corresponding to the diffracting sample can be determined simultaneously by using several XRD line profile analysis methods. One of these methods is the well known procedure of Warren and Averbach,<sup>3</sup> which is based on the analysis of the Fourier coefficients. Another method, such as the Voigt function method,<sup>4</sup> is based on a simplified procedure in which the size and strain parameters can be extracted from the precise XRD pattern of a single peak. This method has been applied to mullite obtained by annealing of kyanite and with two different morphologies. Thus, it is possible to correlate mullite crystallite size and factors that governs this parameter with the grain growth of mullite.

## 2 Experimental Procedure

### 2.1 Material

Experiments were carried out on raw kyanite samples with prismatic shape from northern Spain. The chemical composition (Table 1) was determined by sequential inductively coupled atomic plasma emission spectroscopy (ICP).

### 2.2 Annealing

Kyanite was cut into samples with 10 × 5 × 5 mm<sup>3</sup> dimensions and treated at different temperatures between 1200 and 1600°C for 1–4 h, at a heating rate of 20°C/min. The samples were brought to

**Table 1.** Chemical composition of kyanite (wt%)

Oxides	Raw kyanite	Calcined kyanite
Weight loss (1000°C)	0.59	—
Al <sub>2</sub> O <sub>3</sub>	61.74	62.11
SiO <sub>2</sub>	36.14	36.36
Fe <sub>2</sub> O <sub>3</sub>	0.49	0.50
TiO <sub>2</sub>	0.04	0.04
MnO	0.02	0.02
CaO	0.21	0.21
MgO	0.12	0.12
Na <sub>2</sub> O	0.15	0.15
K <sub>2</sub> O	0.48	0.49

the required temperatures and were quenched to room temperature after appropriate time. The samples were polished down 1  $\mu\text{m}$ , thermally and chemically etched and studied by reflected light optical microscopy (RLOM) and scanning electron microscopy (SEM).

Dilatometric study of kyanite was performed using dilatometer equipment (Adamel-Lhomargy, Paris, France), at a constant heating rate of 5°C/min in air from 20 to 1550°C.

### 2.3 X-ray diffraction measurements

Samples of kyanite treated at 1350 and 1600°C were purified by an acid-leaching technique<sup>5</sup> and studied by XRD. Mullite was identified by XRD powder methods and indexed with the space group *Pbam* with  $a = 7.5451 \text{ \AA}$ ,  $b = 7.689 \text{ \AA}$  and  $c = 2.884 \text{ \AA}$ . The X-ray measurements were made using a conventional Siemens D-500 diffractometer operating at 50 kV and 30 mA, interfaced to an IBM-PC running the Socabim PC software package DIFFRAC-AT. The characteristic reflections of mullite 110, 120, 210, 001, 220, 111 and 121 were selected for the line profile analyses performed on slow recordings of powder samples. Ni-filtered Cu  $K\alpha$  radiation was used. The experimental conditions for data collection were as follows: step width of 0.025°  $2\theta$  and step times of 1.5 and 4 s were used in fast recordings for phase identification; step width of 0.005°  $2\theta$  and variable measurement time (depending on the intensity of the peak) ranging from 25 to 36 s in XRD patterns for line profile analysis.

The line profile analyses of selected reflections of mullite were performed by using the program FIT, available in the software package DIFFRAC-AT. The experimental profiles were fitted to analytic functions (pseudo-Voigt and split-Pearson VII) after subtraction of an adjusted linear background and taking into account the effect of Cu  $K\alpha_2$  component on the experimental profile. The parameter used to estimate the goodness of fit was  $R_{\text{pf}}$  ( $R$ : reliability, pf: profile fitting) defined as:

$$R_{\text{pf}} = \left[ \frac{\sum (I_{\text{obs}} - I_{\text{calc}})^2}{\sum I_{\text{obs}}^2} \right]^{0.5} \cdot 100 \quad (1)$$

where  $I_{\text{obs}}$  and  $I_{\text{calc}}$  are the observed and calculated intensity<sup>5</sup> respectively.

The initial data used in the application of the Voigt function and Warren–Averbach methods were obtained from the profiles fitted to analytical functions. The Warren–Averbach method has been applied by using the program WIN-CRY-SIZE, supplied by Siemens. Two orders of the same reflection are needed for the application of this method, so we have used 110 and 220 reflections in order to evaluate crystallite size in [110] direction and that has been possible because these reflections are intense and relatively isolated (no overlapping with other peaks). For the other directions, there are not two orders of reflection corresponding to intense peaks and without interference with other reflections so the Voigt function method was used since it requires only one peak for the microstructural analysis.

Standard profiles, needed for the evaluation of instrumental line broadening in selected XRD patterns, were obtained from purified mullite obtained from kyanite by firing at 1700°C (2 h) and free of glassy phase by acid leaching. XRD patterns of these standards were recorded separately under the same experimental conditions mentioned above.

### 2.4 Methods of line profile analysis

#### 2.4.1 Warren-Averbach<sup>3</sup>

This method is based on the analysis of the coefficients of the Fourier series that describe the XRD profiles, and it is usually combined with the Stokes deconvolution procedure (that also is an analysis method of Fourier) in order to remove all effects of instrumental broadening from the experimental profiles.

The coefficients of the cosine terms of the Fourier series that describes the diffraction peak can be expressed as a two factors product, according to:

$$A(n, l) = A^{\text{S}}(n) A^{\text{D}}(n, l) \quad (2)$$

where:  $n$  = harmonic number of the Fourier coefficients, and  $l$  = order of the reflection.

The  $A^{\text{S}}(n)$  term contains only information relative to the domains size, while the term  $A^{\text{D}}(n, l)$  contains information related to the lattice microstrains. If there are at least two orders of the same reflection (e.g. 002 and 004, 111 and 222) it is possible to separate the contributions to the peak broadening produced by domain size and strains by using the following relationship:

$$\ln [A(n,l)] = \ln [A^s(n)] - 2\pi^2 \langle \epsilon^2(n) \rangle n^2 l^2 \quad (3)$$

where the parameter  $\epsilon(n)$  represents the micro-strain related to the length,  $L$ , of a column of unit cells, that is to say  $\epsilon(n) = \Delta L/L$ . Since the  $\epsilon(n)$  values can be positive as well as negative, the parameter that is determined is  $\langle \epsilon^2(n) \rangle$ , averaged to all the columns of the domains (crystallites) of the sample.

If now, it is represented  $\ln[A(n,l)]$  versus  $l^2$ , the  $A^s(n)$  coefficients are obtained for several  $n$  values. From these coefficients, as can be demonstrated, it is possible to obtain the average thickness of the diffraction domains through this relationship:

$$\left[ \frac{dA^s(n)}{dn} \right]_{n \rightarrow 0} = - \frac{1}{\langle D_s \rangle} \quad (4)$$

Thus, the value of  $\langle D_s \rangle$  can be obtained from the initial negative slope of  $A^s(n)$  versus  $n$  (or  $L$ ) and represents the average length of the domain columns perpendicular to the reflecting planes  $hkl$ . The parameter  $\langle D_s \rangle$  represents in fact an 'effective' size, since it is related to the broadening contribution not only by the domain size, but additional effects such as faulting and twinning.

Concerning microstrains, the term  $\langle \epsilon^2(n) \rangle$  was obtained for each  $n$  value from the slopes of the graphs  $\ln[A(n,l)]$  versus  $l^2$ . A value that tends to be employed to characterize microstrain is  $\langle \epsilon^2(n) \rangle^{1/2}$  (root mean square strain, abridged RMS).

#### 2.4.2 Voigt function<sup>4</sup>

This method is a single peak procedure. The diffraction profile is assumed to be Voigtian (convolution of Cauchy and Gaussian profiles) because it has been proved that the real diffraction profiles are well adjusted to the Voigt function.<sup>7</sup> The Cauchy and Gaussian components of the measured profiles are related with microstructural parameters (size and strain) of the diffracting sample. So these components must be calculated by using these empirical formulae:<sup>8</sup>

$$\beta_C = \beta [2.0207 - 0.4803\Phi - 1.7756\Phi^2] \quad (5)$$

$$\beta_G = \beta [0.6420 + 1.4187(\Phi - 2/\pi)^{0.5} - 2.2043\Phi + 1.8706\Phi^2] \quad (6)$$

where  $\Phi = 2\omega/\beta$  ( $\beta$ : integral breadth of the profile,  $2\omega$ : full width at half the maximum intensity). The parameter  $\Phi$  is indicative of the composition of the experimental profile. If  $\Phi = 0.63662$ , the profile is totally Cauchyan, while  $\Phi = 0.93949$  corresponds to a totally Gaussian profile. The method of the Voigt function can be employed when the parameter of the profile is found among the two indicated limits.

Once  $\beta_C$  and  $\beta_G$  are known for experimental profiles, the true broadened profile can be found

after subtraction of instrumental broadening which is obtained from the  $\beta_C$  and  $\beta_G$  values of standard profile used. The following equations are applied:

$$\beta_{Cf} = \beta_{Ch} - \beta_{Cg} \quad (7)$$

$$(\beta_{Gf})^2 = (\beta_{Gh})^2 - (\beta_{Gg})^2 \quad (8)$$

where the subscripts f, h and g refer respectively to true, experimental and standard broadened profiles.

The Cauchy component of the f profile is assumed to be only due to the crystallite size effect which then is given by:

$$\langle D_v \rangle = \frac{\lambda}{\beta_{Cf} \cos \theta} \quad (9)$$

On the other hand, the strain is given by:

$$e = \frac{\beta_{Gf}}{4 \tan \theta} \quad (10)$$

$\beta$  is expressed in rad,  $\lambda$  is the wavelength of the radiation used and  $\theta$  is the Bragg angle for the  $\alpha_1$  component.

### 3 Results and Discussion

The thermal transformation of the kyanite samples was studied by dilatometry (Fig. 1) from room temperature to 1550°C using a constant heating rate of 5°C/min and the crystalline phases present were determined by XRD. In Fig. 1, the various stages of transformation and liquid formation during the thermal treatment are shown. The first stage, defined by temperatures below 1320°C (a) corresponds to the starting of the kyanite  $\rightarrow$  mullite + silica transformation. The reaction starts at grain boundaries and cleavage planes of kyanite and produces fibrous mullite aggregates (Fig. 2) The second stage, defined by temperatures between 1320° and 1420°C (a–b) is associated with the progress of the reaction leading to the total transformation at 1420°C. This fact was confirmed by XRD studies (Fig. 1) showing the complete conversion of kyanite into mullite + silica in the temperature range 1350–1420°C. Finally, at temperatures above 1420°C (c) a slight contraction was observed in the material, attributed to the formation of liquid phase due to the presence of minor impurities.

The XRD studies confirmed the development of the above-mentioned reaction and transformation sequence. It should be noted that cristobalite phase, which may have formed, was not detectable during the thermal transformation of kyanite. This is in contrast to the data found in the literature.<sup>9</sup> This is probably due to the presence of minor impurities

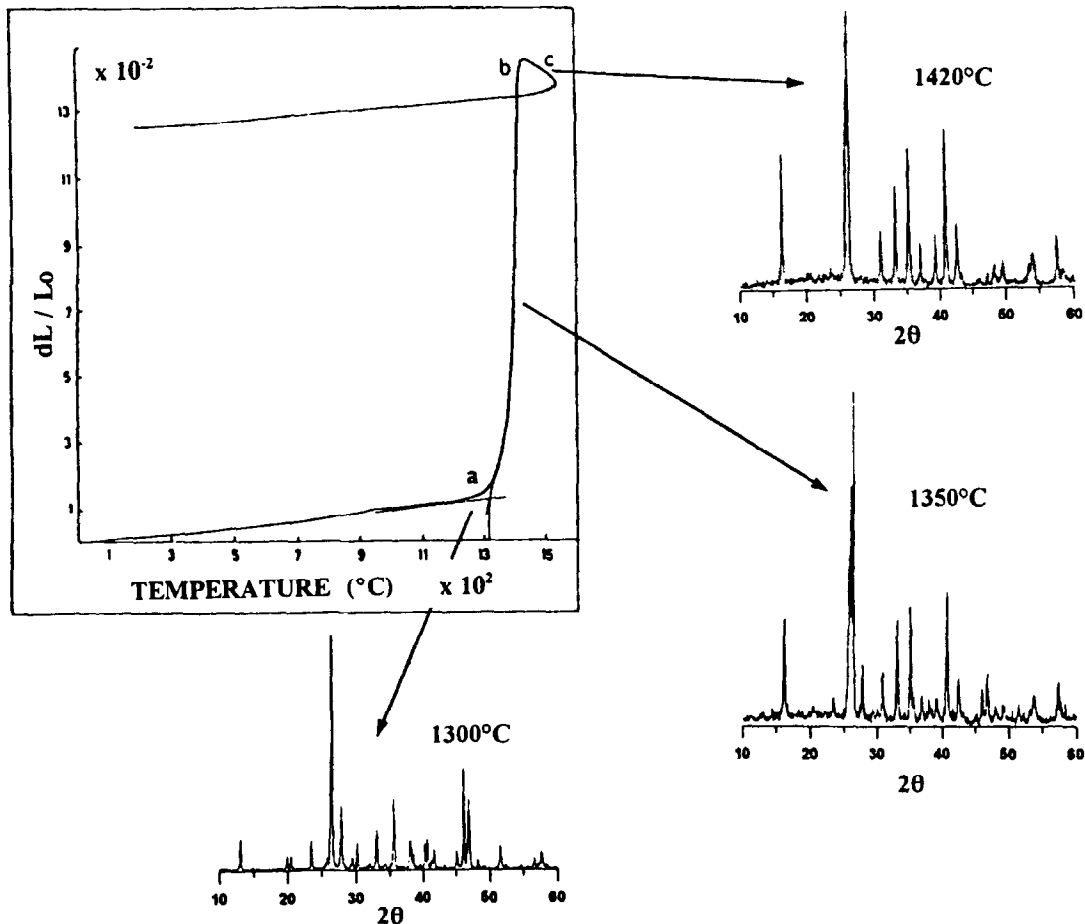


Fig. 1. Dilatometry of raw kyanite.

which formed a liquid phase at the temperature of cristobalite nucleation (1350–1400°C). As a result, all free silica generated at high temperatures during the transformation goes into the liquid phase.

Morphology evolution of the mullite grains generated during the transformation process was studied at temperatures between 1200 and 1600°C by SEM.

At 1200°C (Fig. 2), needle-like mullite grains were observed on the surface of the kyanite particles and in areas close to the grain boundary or on the crack surfaces generated during the transformation reaction. This indicates that the transformation probably started at temperatures below 1200°C. This is in good agreement with the previously published results.<sup>10</sup> Nevertheless, the average extent



Fig. 2. SEM micrograph showing needle-like mullite grains developed during thermal transformation of kyanite at 1200°C.



Fig. 3. SEM micrograph of kyanite showing acicular aggregates of mullite at 1350°C.



Fig. 4. SEM micrograph showing 'tabular' shape mullite grains at 1600°C.

of the transformation at this temperature was very small and, therefore, undetectable by dilatometry and X-ray diffraction technique.

At temperatures between 1200 and 1350°C (Fig. 3) the transformation always produced needle-like mullite grains, showing fine-fibrous aggregates having a preferred orientation along the direction of elongation of crystals. This has been attributed to lower interfacial energies of crystal faces parallel to the  $c$  axis direction<sup>10</sup> (coincident with the elongation direction of crystals). On the other hand, no appreciable change in the size and aspect ratio of the grains was observed within this range of temperature. The grain size mostly varied between  $2.6 \pm 0.5 \mu\text{m}$  long and  $0.25 \pm 0.05 \mu\text{m}$  width, with an aspect ratio value of  $11.2 \pm 0.5$  at 1250°C.

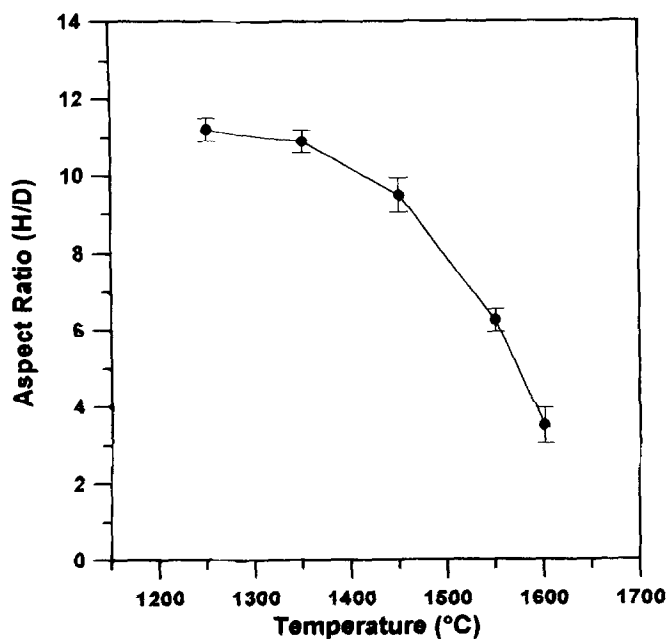


Fig. 5. Aspect ratio evolution of mullite grains as a function of the temperature of treatment of kyanite, determined by SEM.

At temperatures higher than 1350°C, the morphology of the mullite grains was altered strongly and the crystals showed rectangular faces with rounded ends (Fig. 4). The apparent size of the faces in the grains varied between  $3.2 \pm 0.5 \mu\text{m}$  long and  $0.9 \pm 0.1 \mu\text{m}$  wide with a noticeable decrease of the aspect ratio value to  $3.5 \pm 0.5$  at 1600°C. The size and the aspect ratio of the mullite grains as a function of temperature are shown in Figs 5 and 6 respectively.

The methods of XRD line profile analysis mentioned previously were used for the microstructural characterization of mullite contained in the kyanite fired at 1350 and 1600°C for 4 h. Table 2 shows the parameters of the studied profile lines. The results corresponding to the microstructural analysis are given in Table 3. It can be seen how the average size of crystallites of mullite ( $\langle D_v \rangle$  or  $\langle D_s \rangle$ ) increases with the temperature. The data corresponding to the Voigt function method reveal that there are increases in crystallite size along several crystallographic directions. On the other hand, simultaneously, the parameters that indicate reticular distortions ( $\epsilon$  or RMS) decrease in the sample obtained at the higher temperature.

Taking into account the evolution of these two kinds of parameter (size and strain), the mullite obtained at 1600°C has a high degree of crystallinity if this sample is compared with that obtained at 1350°C. This fact is shown by both methods of XRD line profile analyses, although the direct comparison between  $\langle D_v \rangle$  and  $\langle D_s \rangle$  values is not possible because these parameters have different significance. Generally, the  $\langle D_s \rangle$  values were found to be higher than  $\langle D_v \rangle$ .<sup>10</sup>

Comparing the SEM values of  $D$  (width) observed at 1350°C and 1600°C (Fig. 6) with the  $D_v$  values for prismatic planes (range from 0.07 to 0.13  $\mu\text{m}$  at 1350°C to 0.11–0.28  $\mu\text{m}$  at 1600°C, Table 3) and comparing the SEM values of  $H$  (length) observed at 1350 and 1600°C (Fig. 6) with the  $D_v$  values for pinacoidal or bipyramidal planes (range from 0.09 to 0.17  $\mu\text{m}$  at 1350°C to 0.11–0.26  $\mu\text{m}$  at 1600°C, Table 3), it is possible to obtain the number of crystallites in the different directions ( $D/D_v(hk0)$  and  $H/D_v(hkl)$   $l \neq 0$ ).

It can be deduced that at 1350°C the number of crystallites in the direction of the grain elongation (17–32.2) is significantly higher than the number of crystallites in perpendicular directions to the grain elongation (2–3.7). At 1600°C no increase in the number of crystallites along the elongation direction  $H$  (12–29) was detected but an increase was observed in perpendicular directions (3.1–7.3).

This results suggest that at 1350°C the crystallites may be located in such a manner as to cause the elongation along the grain according to the

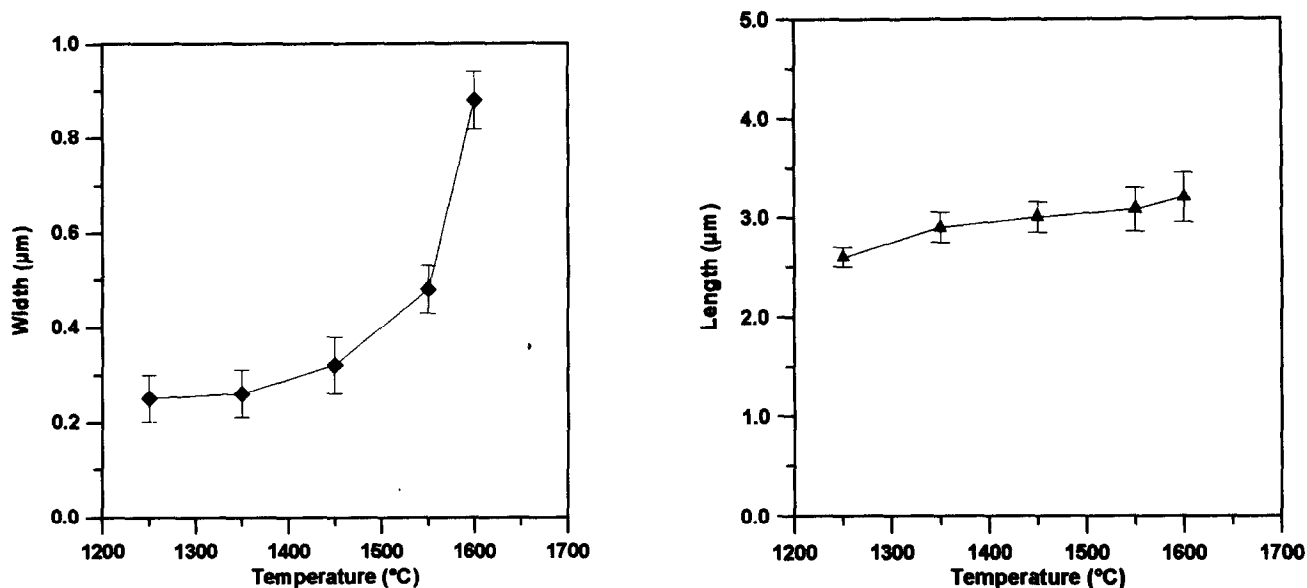


Fig. 6. Evolution of length and width of mullite grains versus temperature, determined by SEM.

Table 2. Parameters obtained by using the fitting procedure of XRD peaks that has been performed previously to the microstructural analysis.

hkl	Mullite LT:1350°C			Mullite HT:1600°C		
	$R_p(\%)$	$2\theta_{obs}(\circ)$	$2\omega(\circ)$	$R_p(\%)$	$2\theta_{obs}(\circ)$	$2\omega(\circ)$
110	8.72	16.391	0.1851	10.88	16.390	0.1650
120	3.31[4]	25.989	0.2026	4.13[2]	25.989	0.1597
210	3.31[4]	26.293	0.1921	4.13[2]	26.294	0.1378
001	4.96	30.982	0.1589	6.03	30.983	0.1382
220	4.67	33.169	0.2152	5.05	33.191	0.1589
111	4.41[2]	35.262	0.2048	6.58	35.273	0.1570
121	5.37[2]	40.854	0.2155	4.14	40.877	0.1527

In all cases a pseudo-Voigt function has been used in the line profile analysis. The number of peaks involved in the fitting procedure is indicated in parentheses.

Table 3. Microstructural parameters of mullites evaluated from XRD line profile analysis and corresponding to samples obtained by thermal transformation of kyanite at low and high temperature (LT and HT respectively)

Single line procedure (Voigt function)				
hkl	Mullite LT:1350°C		Mullite HT:1600°C	
	$\langle Dv \rangle (\text{Å})$	$e \cdot 10^2$	$\langle Dv \rangle (\text{Å})$	$e \cdot 10^2$
110	1143	0.265	1480	0.207
120	1257	0.186	2842	0.111
210	1070	0.186	2725	0.100
001	1705	0.143	1565	0.086
220	776	0.181	1279	0.109
111	950	0.170	1181	0.093
121	1313	0.150	2636	0.067
Multiple-line analysis (Warren-Averbach)				
hkl	Mullite LT:1350°C		Mullite HT:1600°C	
	$\langle Ds \rangle (\text{Å})$	$RMS_{(L=50\text{Å})} \cdot 10^2$	$\langle Ds \rangle (\text{Å})$	$RMS_{(L=50\text{Å})} \cdot 10^2$
110-220	1045	0.243	1173	0.181

Table 4. Aspect ratio of possible faces in different combinations of forms obtained from apparent XRD crystallite sizes.

Combinations of forms	Present forms	Temperature (°C)	H/D of possible faces		
			210	110	120
a	{110}+{001}	1350	n.p <sup>a</sup>	2.35	n.p
		1600	n.p	1.07	n.p
b	{001}+{110}+{120}	1350	n.p	2.0	6
		1600	n.p	1.02	w.m.e <sup>b</sup>
c	{001}+{110}+{210}	1350	3.27	2.88	n.p
		1600	2.88	0.8=	n.p
d	{001}+{110}+{210}+{120}	1350	3.1	8.25	6.1
		1600	w.m.e	0.95 =	w.m.e
e	{110}+{001}+{111}	1350	n.p	0.44 =	n.p
		1600	n.p	1/2.27	n.p
				0.32 =	n.p
				1/3.12	

<sup>a</sup>n.p - Not present in this combination.

<sup>b</sup>w.m.e - Without morphological expression.

[001] direction, in other words along the  $c$  axis, while at 1650°C crystallites may be located in such a manner as to cause growth in the perpendicular direction to the grain elongation direction.

Table 4 shows the  $H/D$  values corresponding to prismatic faces of mullite crystallites obtained by XRD. Different combinations of forms are considered assuming that the forms indicated in the second column from the left are present in the crystallites. The corresponding morphologies were obtained by means of the Dowty<sup>12</sup> program, whose starting values were the mullite crystallographic parameters and the  $D_v$  values (see Table 3) used as central distances of the faces. The (110) face (always present) is the face with greater morphological expression, in agreement with the fact that [110] is the direction with lower growth rate of crystallite in mullite.<sup>13,14</sup> It must be noted that  $H$  represents a measurement parallel to [001] direction, while the  $D$  parameter corresponds to a measurement perpendicular to this direction. In all cases, the observed  $H/D$  values were greater for samples obtained at 1350°C, compared with 1600°C. Values near 1 or lower than 1 are found for the 1600°C sample, indicating that in that case the crystallite does not show elongation along the [001] direction, and this has been interpreted<sup>14</sup> as indicative of a tabular-equidimensional crystallite morphology. The greater similarity between  $H/D$  obtained in X-ray crystallites and in SEM particles has been found considering the combination  $d$  ( $\{001\} + \{110\} + \{210\} + \{120\}$ ) of Table 4.

The different stages during growth of mullite crystals were analysed on the basis of the studies carried out. At the beginning of the reaction and until 1350°C, needle-like mullite grains are formed directly from kyanite crystals and no change in mullite morphology was observed by XRD or SEM. The presence of silica coating needle-like mullite grains is the reason proposed<sup>9</sup> to avoid the growth of mullite grains during the decomposition of kyanite at this temperatures.

At temperatures higher than 1350°C, silica goes into a liquid phase by the presence of impurities, thereby allowing the growth of the mullite grains. An important change in the morphology of the mullite grains was observed with decrease of length/width ratio of faces with the temperature (Fig. 5). This can be explained by the fact that at the beginning of the decomposition of kyanite, there is a great number of randomly distributed mullite aggregates. These aggregates grow easily in the natural direction of elongation in crystals. Finally the extension of aggregates is achieved by expanding in the other directions.<sup>15</sup> This effect is enhanced at elevated temperatures due to a decrease in viscosity of the glassy phase with rising temper-

ature. Thus, a rapid diffusion and growth of the crystals take place; then mullite grains become better formed straight-sided prominences with increase in width size. As a consequence, an important decrease in the aspect ratio of mullite grains as a function of temperature takes place (Fig. 5).

Comparing the values given in Table 4 and the values shown in Fig. 5, an agreement of higher values of aspect ratio is obtained at lower temperatures in both techniques. The evolution towards 'tabular' shapes of the average crystallite at high temperature determined by XRD is in agreement with the morphological characteristics of the mullite aggregates observed by SEM at high temperature (Fig. 4).

Finally, the microstructural evolution is in good agreement with the model of Aksay *et al.*<sup>16</sup> in which it is shown that a mullite microstructure with high aspect ratio and random distribution changes during thermal treatment to a microstructure where the grains showed a low aspect ratio. In particular, this model considers the shape of equivalent average grain as a function of aspect ratio, degree of orientation and size distribution of component grains in a microstructure.

#### 4 Conclusions

Mullite crystals formed from kyanite reaction showed two different morphologies. From 1200 to 1350°C the transformation always produces fibrous aggregates of needle-like mullite crystals and no appreciable change in the aspect ratio of the crystals was observed by SEM. Nevertheless, the average extent of the transformation at 1200–1250°C was very small making it undetectable by dilatometry or X-ray techniques. At temperatures higher than 1350°C, the morphology of the mullite grains was altered and at 1600°C the crystals showed rectangular faces with rounded ends. So, the results obtained showed that acicular or rounded end platelet mullite grains of controlled size could be obtained with composition close to theoretical mullite from kyanite as a function of temperature.

XRD line profile analysis and SEM were used to monitor the evolution of average crystallite size and mullite grain aggregates respectively. The variations of the mean apparent crystallite size in different directions have been used for monitoring the evolution of average crystallite size and shape of the mullite aggregates. Column-shaped crystallites characterize the initial stages of the nucleation and growth process but this shape is lost for more developed firing conditions. So morphology reflects a preferential growth of crystals along the

*c* direction (higher number of crystallites along [001] direction) at lower temperatures but growth of crystal along *c* perpendicular direction, generated equidimensional mullite grains at higher temperatures.

The results suggest that, during annealing, the growth of crystallites and aggregates of mullite grains takes place simultaneously. The agreement of aspect ratio between prismatic crystallites and coarser aggregates could be indicative of parallel growth of crystallites in aggregates.

### Acknowledgement

This work was supported by C.I.C.Y.T, Spain under Contract No. MAT.91-0499., MAT. 93-0126

### References

- Schneider, H., Okada, K. and Pask, J. A., *Mullite and Mullite Ceramics*. John Wiley and Sons, Chichester, 1994, pp. 1-251.
- Sacks, M. D., Lee, H. and Pask, J. A., Mullite and mullite matrix composites. In *Ceramics Transactions*, vol. 6, ed. S. Somiya, R. F. Davis and J. A. Pask. Am. Ceram. Soc., Westerville, OH, 1990, pp. 167-207.
- Warren, B. E. and Averbach, B. C., The effect of cold-work distortion on X-ray patterns. *J. Appl. Phys.*, 1950, **21**, 595-599.
- Delhez, R., De Keijser, Th. H. and Mittemeijer, E. J., Determination of crystalline size and lattice distortions through X-ray diffraction line profile analysis. *Fresenius Z. Anal. Chem.*, 1982, **312**, 1-16.
- Wancheng, Z., Litong, Z. and Hengzhi, F., Modification of the hydrofluoric acid leaching technique: Part I. *J. Am. Ceram. Soc.*, 1988, **71**(5), 395-398.
- Will, G., Parrish, W. and Huang, T. C., Crystal-structure refinement by profile fitting and least-squares analysis of powder diffractometer data. *J. Appl. Cryst.* 1983, **16**, 611-622.
- Langford, J. I., A rapid method for analysing breadths of diffraction and spectral lines using the Voigt function. *J. Appl. Cryst.*, 1978, **11**, 10-14.
- De Keijser, Th. H., Langford, J. I., Mittemeijer, E. J. and Vogels, A. B. P., Use of the Voigt function in a single-line method for the analysis of X-ray diffraction line broadening. *J. Appl. Cryst.*, 1982, **15**, 308-314.
- Schneider, H. and Majdic, A., Kinetics of the thermal decomposition of kyanite. *Ceramurgia Intern.*, 1980, **6**, 61-66.
- Johnson, S. M. and Pask, J. A., Role of impurities on formation of mullite from kaolinite and Al<sub>2</sub>O<sub>3</sub>-SiO<sub>2</sub> mixtures. *Am. Ceram. Soc. Bull.*, 1982, **61**(8), 838-842.
- Balzar, D., Profile fitting of X-ray diffraction lines and Fourier analysis of broadening. *J. Appl. Cryst.*, 1992, **25**, 559-570.
- Dowty, E. and Shape, A computer program for drawing crystals. *J. Appl. Cryst.*, 1988, **21**, 211-220.
- Serrano, F. J., Análisis microestructural de mullitas por difracción de rayos X. Ph D thesis, Universidad Valencia, Burjassot, Valencia, Spain, 1995.
- Serrano, F. J., Bastida, J., Amigo, J. M. and Sainz, A., XRD Line broadening studies on mullite. *Cryst. Res. Technol.* 1996, **31**(8), 1085-1093.
- Sainz, M. A., Obtencion de mullita a partir de la transformación termica de cianita. Ph D thesis, Universidad Autónoma, Madrid, Spain, 1995.
- Hirata, Y. and Aksay, I. A., Grain growth of mullite. Conference paper presented at 94th Annual Meeting of Am. Ceram. Soc., Minneapolis, 1992.